Journal of Science and Technology in Civil Engineering, HUCE (NUCE), 2022, 16 (2): 65–75

OPTIMUM LOCATION OF A SINGLE LONGITUDINAL STIFFENER WITH VARIOUS CROSS-SECTION SHAPES OF STEEL PLATE GIRDERS UNDER BENDING LOADING

George Papazafeiropoulos[a], Quang-Viet Vu[b], Viet-Son Nguyen[c], Viet-Hung Truong[d,*]

[a]*Department of Structural Engineering, National Technical University of Athens, Zografou, Athens 15780, Greece*
[b]*Faculty of Civil Engineering, Vietnam Maritime University, 484 Lach Tray street, Le Chan district, Hai Phong city, Vietnam*
[c]*State Authority for Construction Quality Inspection, Ministry of Construction, 37 Le Dai Hanh street, Hai Ba Trung district, Hanoi, Vietnam*
[d]*Faculty of Civil Engineering, Thuy Loi University, 175 Tay Son street, Dong Da district, Hanoi, Vietnam*

Article history:
Received 01/3/2022, Revised 22/3/2022, Accepted 24/3/2022

Abstract

This paper aims at investigating the optimum location of a single longitudinal stiffener having various cross-section types of steel plate girders subjected to bending loading. The optimum location is found using a gradient-based Interior-Point (IP) optimization algorithm. The optimization procedure involves a linear elastic buckling analysis with the finite element method, which is coupled with the aforementioned IP algorithm and used to calculate the buckling coefficient, which is maximized. Based on the optimization results, the effect of the various cross-section types of the stiffener and the web slenderness ratio on the optimum stiffener position is investigated. It is found that closed cross-sections of the stiffener and larger web slenderness ratios lead to higher critical buckling coefficients.

Keywords: optimum stiffener position; stiffener cross-section, optimization; Abaqus2Matlab; steel plate girders.

https://doi.org/10.31814/stce.huce(nuce)2022-16(2)-06

1. Introduction

In recent years, longitudinal stiffeners have been commonly used in girder webs to eliminate the web crippling failure, which leads to a significant reduction of the resistance of the girder. There are various types of longitudinal cross-sections such as flat, T-shaped, L-shaped, rectangular, triangular, and trapezoidal sections, among others. Numerous researches have been performed to investigate the behavior of the steel plate girder reinforced by longitudinal stiffeners under bending loading, especially for flat stiffeners. Regarding the optimum location of the flat stiffeners, many researchers have reported that it is at $0.2D$ (where D is the web depth of the girder) from the compression flange of the girder with the assumption of simply supported longitudinal edges of the girder web [1–4]. Recently, by using the FE method, several researchers have found that the optimum position of a

*Corresponding author. *E-mail address:* truongviethung@tlu.edu.vn (Truong, V.-H.)

single stiffener for the plate girder is at about $0.42D_c$ (D_c is the web depth in compression in the elastic range) regardless of any asymmetry of the girder section [5–8].

Regarding the optimum location of the stiffener having various cross-section types, based on buckling analysis of the stiffened plate under bending, Maiorana et al. [9] reported that the optimum position of various stiffener types consisting of flat, T-shaped, L-shaped, rectangular, triangular, and trapezoidal section types is at 0.2D regardless of the stiffener type. However, in the study mentioned above, the presence of the girder flange, which may affect the buckling response and its optimum location, has not been taken into consideration.

This work aims to determine the optimum position of a longitudinal stiffener having various cross-section types based on maximizing the critical buckling load of the girder plate at which it is placed under bending loading. A similar optimization procedure proposed by Vu et al. [3, 4] is employed. In addition, the optimized buckling coefficients for the various stiffener cross-section configurations are compared to determine the most effective stiffener cross-section type of the girder under bending.

2. Methodology

2.1. Formulation of the linear elastic buckling problem

In Fig. 1, longitudinally stiffened plate girders having various stiffener cross-section types subject to bending loading, which are considered in this study, are shown. The plate girders are comprised of a web plate, a top flange under compression, and a bottom flange under tension. After the reference load P exceeds a critical value P_{cr}, the web of the plate girder buckles. Linear elastic buckling analysis is performed in this study to estimate the critical load P_{cr}. This analysis is comprised of the following two analyses:

a) A standard linear perturbation static analysis in which a (unit) reference load pattern F is applied to the structure. The stresses and/or loads that are calculated from this static analysis are then used to form the geometric stiffness matrix K_G used in the buckling analysis.

b) The solution of the following eigenvalue problem:

$$(K + \lambda K_G)\, u = 0 \tag{1}$$

where K is the stiffness matrix of the model and λ is the multiplier of the reference load pattern F. Eq. (1) is solved for the lowest positive value of λ, which is the buckling eigenvalue denoted as λ_{cr}, as well as the buckling mode shapes (eigenvectors) u.

After the two above analyses are carried out, the buckling load is calculated by the following equation:

$$F_{cr} = \lambda_{cr} F \tag{2}$$

Besides this, the critical buckling load of a plate girder subject to bending loading can be calculated by a relation adapted from the classical buckling theory of plates under pure compression, as follows:

$$F_{cr} = k_b \frac{\pi^2 E t_w^3}{12\,(1 - \nu^2)\, D} \tag{3}$$

Eqs. (2) and (3) above are used to calculate the buckling coefficient k_b. In Eq. (3), E is the elastic Young's modulus, t_w is the web plate thickness, ν is the Poisson's ratio, and D is the depth of the web plate.

Since only the lowest eigenvalue is required in Eq. (1), the Lanczos eigensolver has been used. Besides, the boundary conditions specified for the applied loads of the static perturbation analysis and the antisymmetry boundary conditions for the buckling modes are identical.

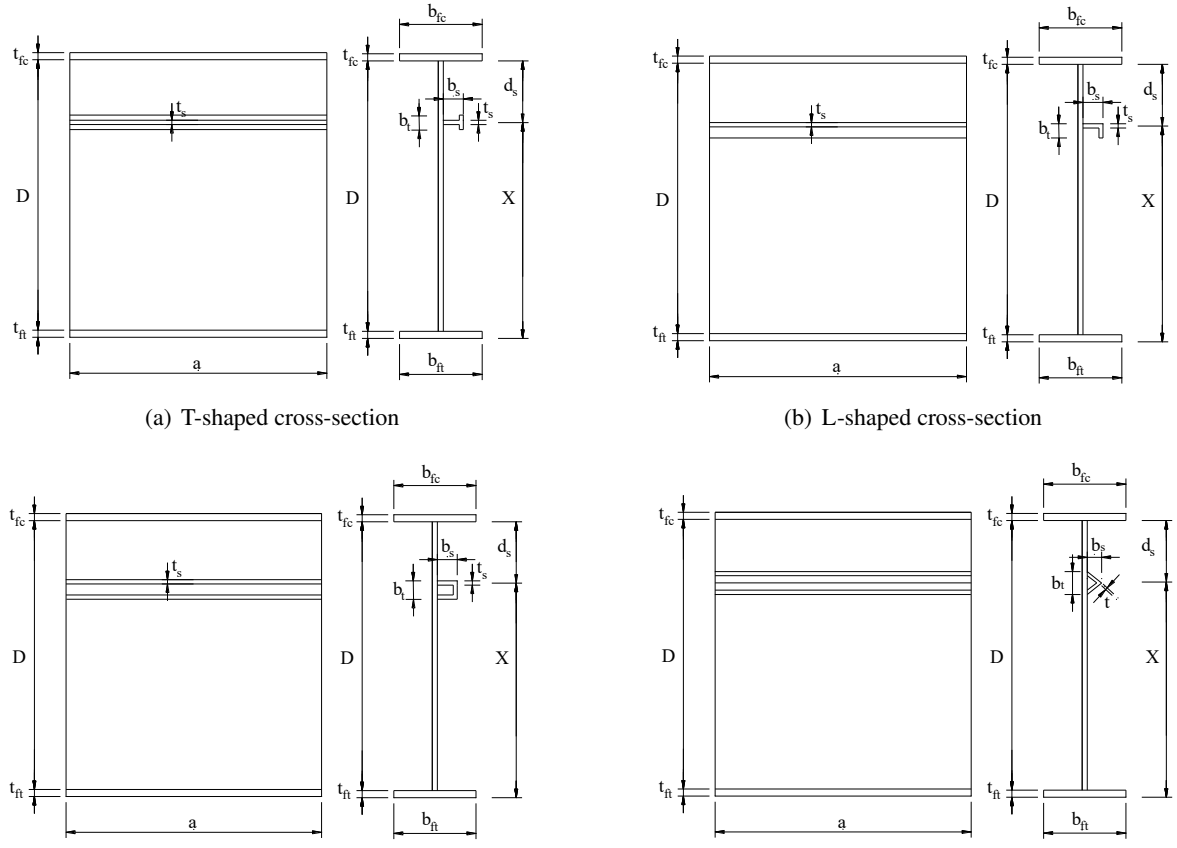

(a) T-shaped cross-section

(b) L-shaped cross-section

(c) Rectangular cross-section

(d) Triangular cross-section

Figure 1. Geometry of longitudinally stiffened plate girders having various stiffener cross-section types

2.2. *Optimization method of longitudinally stiffened plates*

It is generally desired that the plate girder is designed so that its critical buckling load is maximized, and this is the objective of optimizing the stiffener location. Therefore, in this study, the optimum stiffener location is found based on maximizing the bending buckling coefficient k_b. In a more compact form, the optimization problem can be formulated as follows:

Find d_s that maximizes k_b given by Eq. (4):

$$k_b\left(d_S\right) = \frac{12\left(1-\nu^2\right)D}{\pi^2 E t_w^3}\left(F\left(d_S\right)\right)_{cr} \tag{4}$$

subject to the following constraint regarding the stiffener position:

$$0 \leq d_S/D \leq 1 \tag{5}$$

During the above optimization process, it is assumed that the stiffener forms a nodal line at the stiffener-plate junction since this situation corresponds to a much higher buckling coefficient, which is something desirable according to the first optimization step. The condition of nodal line formation is ensured by checking that the out of plane displacements along the nodal line, due to buckling

deformation, do not exceed some nonzero positive tolerance, as follows:

$$r \leq r_{tol} \tag{6}$$

where r_{tol} is the tolerance and the normalized parameter r is given by the relation:

$$r = \frac{\max\left(|w_S|\right)}{\max\left(|w_w|\right)} \tag{7}$$

In Eq. (7), w_S is the out-of-plane displacement of the stiffener and w_w is the out-of-plane displacement of the web plate.

2.3. Optimization procedure

For the solution of the optimization problem formulated in Eqs. (4) to (7), several methods can be used, such as using metaheuristic algorithms [10–12], direct optimization methods [13], etc. In this study, an Interior Point algorithm (IP), one of the robust direct optimization methods, was used [14–16]. This gradient-based algorithm uses direct Newton or conjugate gradient steps to proceed from an initial guess to the optimum solution. The whole optimization procedure has been implemented in Abaqus [17] and Matlab [18], using Abaqus2Matlab [19, 20] as the coupling software that links the two formers. Abaqus2Matlab has been used for integrating Abaqus and Matlab within the optimization loop. The optimization procedure for computing the optimum stiffener location, as mentioned in Section 2.2, is presented in Fig. 2. Detailed steps of this procedure are described below:

Step 1: Define the design parameters/variables of the optimization problem.

Step 2: Build a Matlab function that accepts the design parameters (variables) as input and automatically generates the corresponding Abaqus input file (*inp) of the model.

Step 3: Define and build the objective function of the optimization problem.

Step 4: A main Matlab code is constructed, including the initial guess for the solution, lower bound and upper bound values, and optimization algorithm (Matlab nonlinear programming solver *fmincon* using the IP algorithm).

Step 5: The objective function is evaluated. The Abaqus input file is created in Matlab and run by Abaqus (inside Matlab). After the Abaqus analysis is completed, the results are loaded in Matlab using Abaqus2Matlab.

Step 6: The optimization procedure using the IP algorithm is implemented.

Step 7: Check if the termination criterion is met. This criterion varies among the various optimization algorithms; however, in this study, limits for the function, step and optimality tolerances were used. If the criterion is satisfied, the process will terminate. Otherwise, go to the next step.

Step 8: A new Abaqus input file is created by changing the design variables' values.

Step 9: The Abaqus analysis is run again.

Step 10: Repeat steps 6-9 until convergence is obtained within the specified tolerance.

Step 11: The values of the design variables at the termination point of the optimization algorithm are accepted as the final solution.

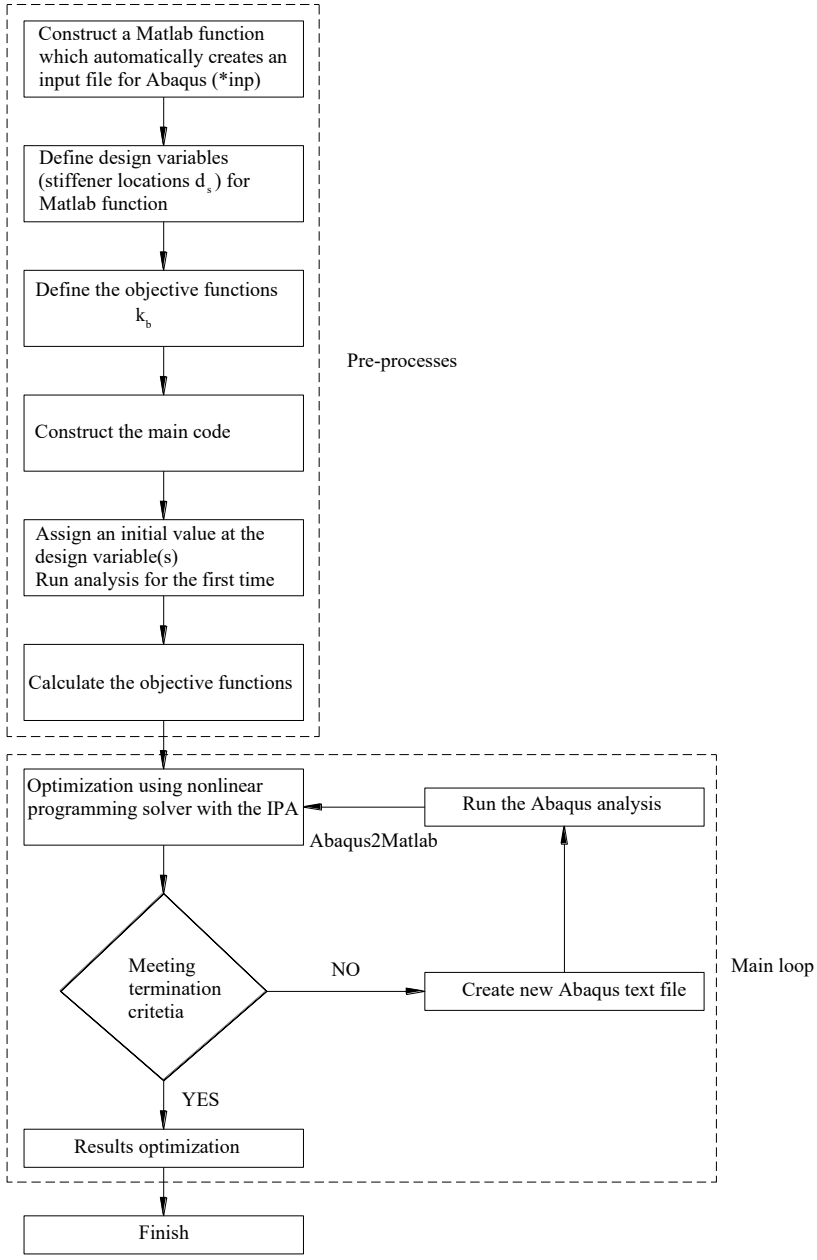

Figure 2. Flowchart of the optimization procedure

3. Finite element simulation

The buckling response of the longitudinally reinforced plate girder shown in Fig. 1 is calculated through FE analysis of the structure. For this purpose, ABAQUS commercial finite element software [17] has been used.

In this study, FE models of the girder having various stiffener cross-sections (T-shaped, L-shaped, triangular, rectangular sections are established based on the FE model of the girder having the flat longitudinal stiffener used in the paper of Vu et al. [7, 8]. All geometric descriptions of the girder

(except the stiffener dimensions), material properties, and modeling procedure are identical to that of the girder having the flat longitudinal stiffener mentioned in the papers of Vu et al. [7, 8]. In particular, the height and thickness of the webs are selected as 3.0 m and 9.0 mm, respectively. The flange width and thickness of the girder are chosen as 600 mm and 54 mm, respectively. The panel aspect ratio

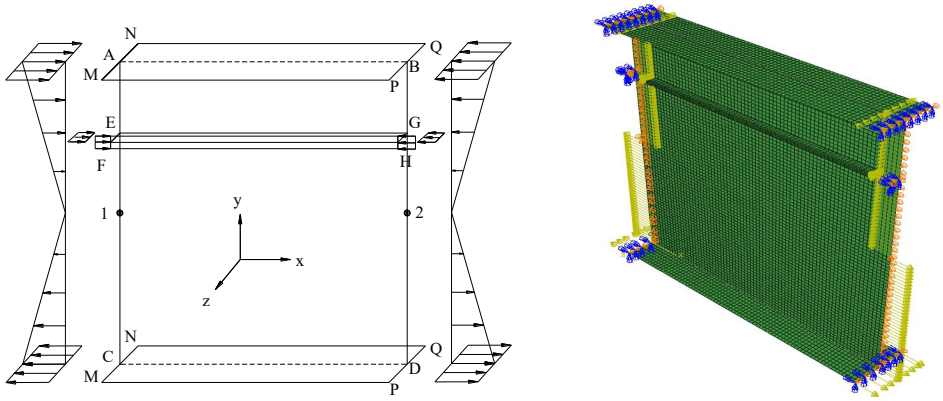

(a) T-shaped cross section

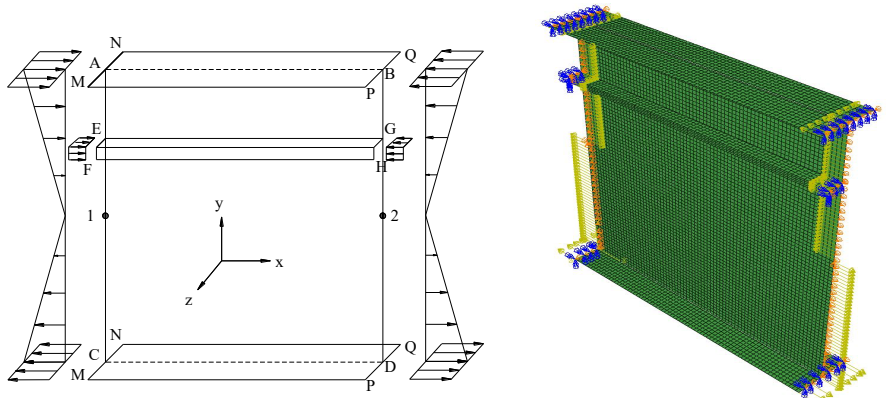

(b) L-shaped cross section

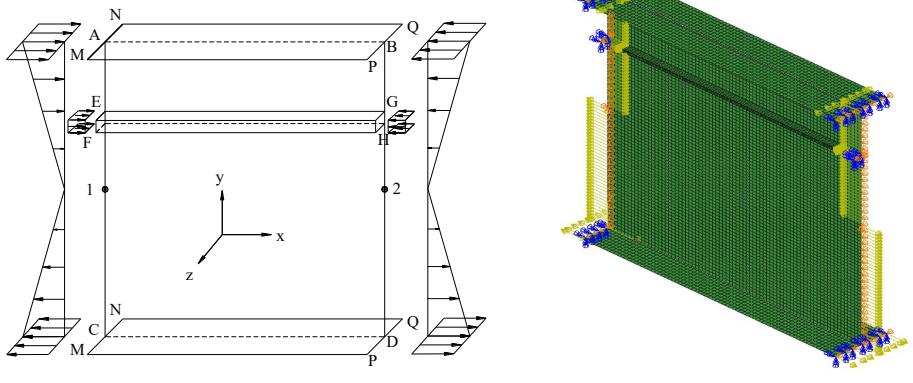

(c) Rectangular cross section

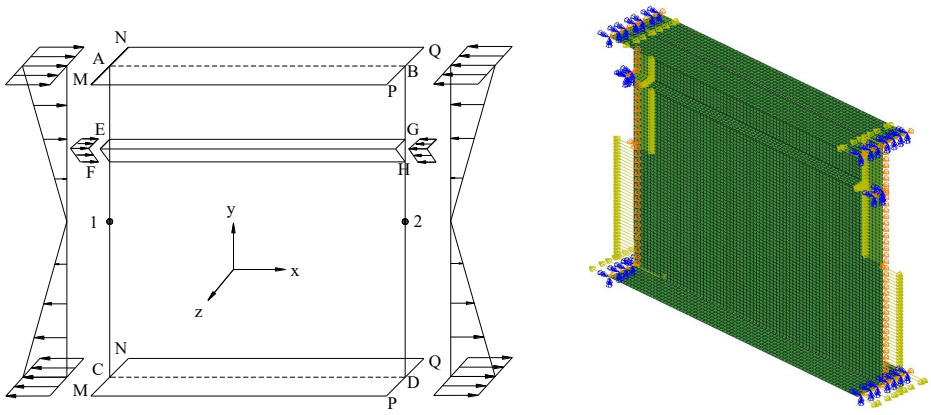

(d) Triangular cross-section

Figure 3. Loading and boundary conditions of different plate girder configurations: (a) T-shaped, (b) L-shaped, (c) Rectangular, (d) Triangular section

(the length–to–depth ratio of the girder) is fixed at 1.0. All materials are linear elastic with Young's modulus and Poisson's ratio $E = 210$ GPa and $v = 0.3$, respectively. It is assumed that vertical edges of the stiffened web plate girder are simply supported. All elements used for the model are simulated by 4-node shell elements S4R which is available on the ABAQUS element library. The mesh size is 40 mm, as mentioned in references [7, 8]. Loading and boundary conditions for different stiffener types are illustrated in Fig. 3.

The efficiency of the FE model of the plate girder having flat longitudinal stiffener has been verified in Vu et al. [7, 8]. In this work, since the geometry, material properties, and modeling procedure of the plate girder with various stiffener cross-section types are identical with those of the girder having flat stiffener (only stiffener shapes are different), the accuracy of these FE models is acceptable. It is noted that the cross-section area of the stiffeners with various cross-section types remains constant for purposes of comparison.

Based on these FE models, the optimum stiffener position of different longitudinal stiffener cross-section types will be determined (based on the procedure mentioned in section 2.3) and presented in section 4 of this work.

4. Optimum location of stiffener having different cross-section types

4.1. Optimum location of various stiffener types

In this section, by using the optimization procedure mentioned in Section 2.3, the optimum location of the longitudinal stiffener having various cross-section types consisting of T-shaped, L-shaped, Rectangular, and Triangular cross-sections, along with the web height of the plate girder subjected to pure bending, is investigated.

The optimum location of the longitudinal stiffener having various cross-section types is displayed in Table 1. It is noted that the aspect ratio ($\varphi = a/D$) and web slenderness ratio (D/t_w) are fixed as 1 and 333, respectively, for all stiffener types. It can be seen from Table 1 that the optimum location of stiffeners is around $0.2D$ regardless of the cross-section type. This result is similar to Maiorana et al. [9] for stiffened plates. It means that the stiffener type does not significantly affect the optimum

stiffener location regardless of stiffened plates and stiffened plate girder under bending. In addition to the above, it is apparent that k_b of the stiffener with rectangular cross-section is maximum while kb of the stiffener with T-shaped is minimum. It is also seen that the k_b of the stiffeners with closed cross-sections is much higher than with open cross-sections. Therefore, using stiffeners with closed cross-sections significantly improves the buckling resistance of the girder compared to stiffeners with open cross-sections. Fig. 4 shows the convergence history, while Fig. 5 shows the buckling mode shapes of the stiffened plate girder under bending for the various stiffener cross-section types. It can be observed from Fig. 5 that the mode shapes of the part of the girder web under the stiffener are similar regardless of the stiffener type.

Table 1. Optimization results for the longitudinal stiffener with various cross-section types

Stiffener type	φ	λ_w	d_s/D	d_s/D_c	k_b
T-shaped	1	333	0.202	0.404	215.88
L-shaped	1	333	0.202	0.404	220.59
Rectangular	1	333	0.197	0.394	303.24
Triangular	1	333	0.199	0.399	291.34

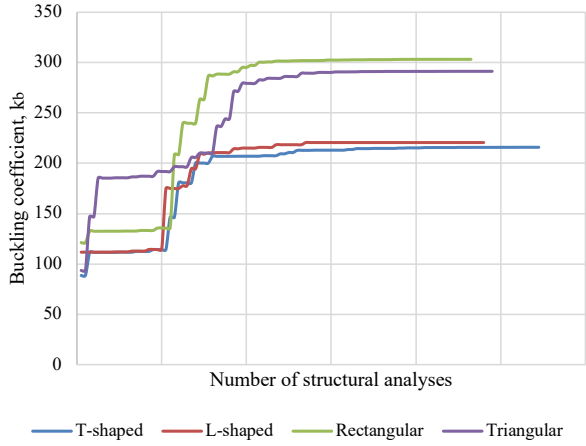

Figure 4. Convergence history for the various stiffener cross section types

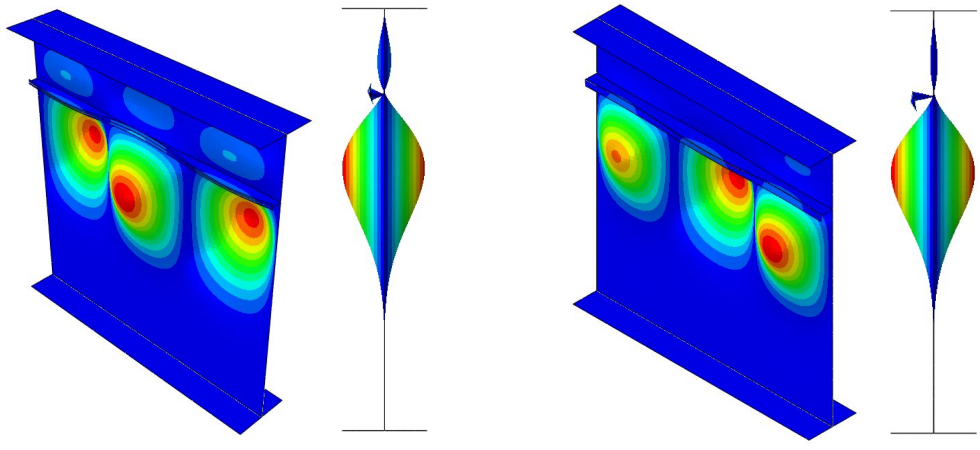

(a) T-shaped (b) L-shaped

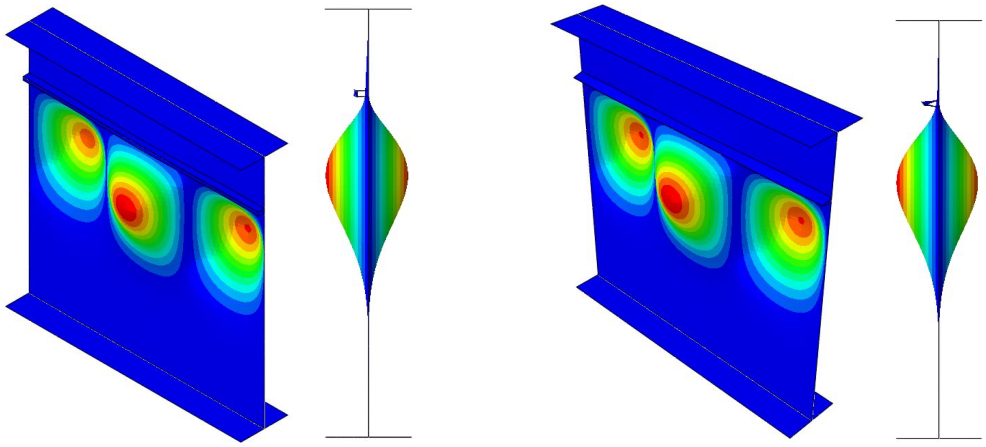

(c) Rectangular (d) Triangular

Figure 5. Buckling mode shapes of the plate girder for the various types of stiffener cross-section

4.2. Effect of web slenderness on the buckling response of the stiffened girder

To investigate the effect of the web slenderness ratio on the buckling response of the stiffened plate girder, different web slenderness ratios of 200, 300, and 333 are considered while the other parameters are fixed. The results are shown in Table 2 and Fig. 6. It can be seen from Table 2 that λ_w has a low effect on the optimum stiffener location for all stiffener types. When λ_w changes, the optimum stiffener location remains roughly equal to $0.2D$ for all stiffeners considered. In addition, it is observed that k_b is reduced when λ_w decreases.

Table 2. Effect of web slenderness ratio on the buckling response of the stiffened girder

λ_w	φ	Stiffener type	d_s/D	d_s/D_c	k_b
333	1	T-shaped	0.202	0.404	215.88
	1	L-shaped	0.202	0.404	220.59
	1	Rectangular	0.197	0.394	303.24
	1	Triangular	0.199	0.399	291.34
300	1	T-shaped	0.203	0.406	213.54
	1	L-shaped	0.203	0.406	216.80
	1	Rectangular	0.197	0.394	298.52
	1	Triangular	0.199	0.398	291.34
200	1	T-shaped	0.205	0.41	198.38
	1	L-shaped	0.205	0.41	199.72
	1	Rectangular	0.199	0.398	279.08
	1	Triangular	0.199	0.398	269.72

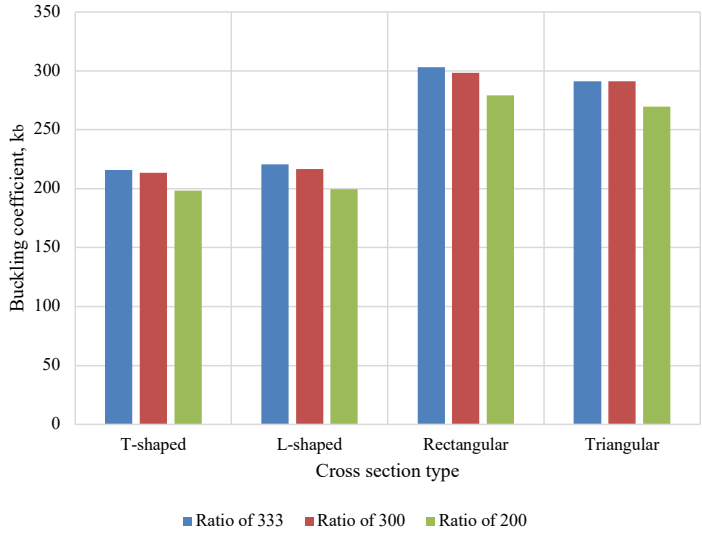

Figure 6. Effect of web slenderness ratio on the buckling response of the stiffened girder

5. Conclusions

In this study, the optimum position of a single longitudinal stiffener with various cross-section configurations at the web of a plate girder subjected to bending loading is investigated, based on buckling analysis with the finite element method. The optimum position is calculated through an optimization procedure implemented in Abaqus and Matlab using Abaqus2Matlab to integrate the two former software into the optimization loop. Optimum results for various stiffener cross-section types consisting of T-shaped, L-shaped, Rectangular, and Triangular cross-sections are obtained. It is found that the optimum stiffener location is approximately at a distance from the compression flange of 20% of the web height, regardless of the stiffener type and the web slenderness ratio. Furthermore, closed cross-sections of the stiffeners lead to a higher critical buckling coefficient than open cross-sections. Moreover, higher values of the web slenderness ratio lead to a higher critical buckling coefficient as well. The effect of other parameters on the optimum stiffener location, such as the aspect ratio, flange slenderness ratio, and stiffener rigidity for the various stiffener cross-section configurations, can be the subject of a future study.

Acknowledgments

This research is funded by Vietnam National Foundation for Science and Technology Development (NAFOSTED) under grant number 107.01-2019.322.

References

[1] Azhari, M., Bradford, M. A. (1993). Local buckling of I-section beams with longitudinal web stiffeners. *Thin-Walled Structures*, 15(1):1–13.

[2] Alinia, M. M., Moosavi, S. H. (2008). A parametric study on the longitudinal stiffeners of web panels. *Thin-Walled Structures*, 46(11):1213–1223.

[3] Vu, Q.-V., Papazafeiropoulos, G., Graciano, C., Kim, S.-E. (2019). Optimum linear buckling analysis of longitudinally multi-stiffened steel plates subjected to combined bending and shear. *Thin-Walled Structures*, 136:235–245.

[4] Vu, Q.-V., Truong, V.-H., Papazafeiropoulos, G., Graciano, C., Kim, S.-E. (2019). Bend-buckling strength of steel plates with multiple longitudinal stiffeners. *Journal of Constructional Steel Research*, 158:41–52.

[5] Elbanna, A. A., Ramadan, H. M., Mourad, S. A. (2014). Buckling enhancement of longitudinally and vertically stiffened plate girders. *Journal Engineeing and Applied Science*, 61:351–370.

[6] Kim, H. S., Park, Y. M., Kim, B. J., Kim, K. (2018). Numerical investigation of buckling strength of longitudinally stiffened web of plate girders subjected to bending. *Structural engineering and mechanics: An international journal*, 65(2):141–154.

[7] Hoan, P. T., Trung, P. V., Viet, V. Q. (2020). Determination of optimum stiffener location of steel plate girder bridges under bending. *Journal of Science and Technology in Civil Engineering (STCE) - HUCE*, 14(4V):29–38.

[8] Kim, S.-E., Papazafeiropoulos, G., Graciano, C., Truong, V.-H., Do, Q. T., Kong, Z., Vu, Q.-V. (2021). Optimal design of longitudinal stiffeners of unsymmetric plate girders subjected to pure bending. *Ocean Engineering*, 221:108374.

[9] Maiorana, E., Pellegrino, C., Modena, C. (2011). Influence of longitudinal stiffeners on elastic stability of girder webs. *Journal of Constructional Steel Research*, 67(1):51–64.

[10] Truong, V.-H., Hung, H. M., Anh, P. H., Hoc, T. D. (2020). Optimization of steel moment frames with panel-zone design using an adaptive differential evolution. *Journal of Science and Technology in Civil Engineering (STCE) - NUCE*, 14(2):65–75.

[11] Pham, H.-A., Nguyen, D.-X., Truong, V.-H. (2021). An efficient differential-evolution-based moving compensation optimization approach for controlling differential column shortening in tall buildings. *Expert Systems with Applications*, 169:114531.

[12] Truong, V.-H., Nguyen, P.-C., Kim, S.-E. (2017). An efficient method for optimizing space steel frames with semi-rigid joints using practical advanced analysis and the micro-genetic algorithm. *Journal of Constructional Steel Research*, 128:416–427.

[13] Mockus, J., Paulavičius, R., Rusakevičius, D., Šešok, D., Žilinskas, J. (2015). Application of Reduced-set Pareto-Lipschitzian Optimization to truss optimization. *Journal of Global Optimization*, 67(1-2):425–450.

[14] Byrd, R. H., Gilbert, J. C., Nocedal, J. (2000). A trust region method based on interior point techniques for nonlinear programming. *Mathematical Programming*, 89(1):149–185.

[15] Byrd, R. H., Hribar, M. E., Nocedal, J. (1999). An Interior Point Algorithm for Large-Scale Nonlinear Programming. *SIAM Journal on Optimization*, 9(4):877–900.

[16] Waltz, R. A., Morales, J. L., Nocedal, J., Orban, D. (2005). An interior algorithm for nonlinear optimization that combines line search and trust region steps. *Mathematical Programming*, 107(3):391–408.

[17] ABAQUS (2014). *Analysis User's Manual version 6.14*. Dassault Systems.

[18] MathWorks, Inc. (2017). *MATLAB R2017b*.

[19] Papazafeiropoulos, G., Muñiz-Calvente, M., Martínez-Pañeda, E. (2017). *Abaqus2Matlab*.

[20] Papazafeiropoulos, G., Muñiz-Calvente, M., Martínez-Pañeda, E. (2017). Abaqus2Matlab: A suitable tool for finite element post-processing. *Advances in Engineering Software*, 105:9–16.